01 Feb 2017

A Novel Tantalum-Containing Bioglass. Part II. Development of a Bioadhesive for Sternal Fixation and Repair

Adel MF Alhalawani

Cina Mehrvar

Wendy Stone

Stephen D. Waldman

et. al. For a complete list of authors, see https://scholarsmine.mst.edu/che_bioeng_facwork/1104

Recommended Citation

A. M. Alhalawani et al., "A Novel Tantalum-Containing Bioglass. Part II. Development of a Bioadhesive for Sternal Fixation and Repair," *Materials Science and Engineering C*, vol. 71, pp. 401 - 411, Elsevier, Feb 2017.

The definitive version is available at https://doi.org/10.1016/j.msec.2016.10.024

Materials Science and Engineering C 71 (2017) 401–411

Contents lists available at ScienceDirect

Materials Science and Engineering C

journal homepage: www.elsevier.com/locate/msec

A novel tantalum-containing bioglass. Part II. Development of a bioadhesive for sternal fixation and repair

Adel MF. Alhalawani [a,b], Cina Mehrvar [a], Wendy Stone [c], Stephen D. Waldman [b,d], &, Mark R. Towler [a,b,*]

[a] Department of Mechanical & Industrial Engineering, Ryerson University, Toronto, Ontario, Canada
[b] Li Ka Shing Knowledge Institute, St. Michael's Hospital, Toronto, Ontario, Canada.
[c] Department of Chemistry and Biology, Ryerson University, Toronto, Ontario, Canada
[d] Department of Chemical Engineering, Ryerson University, Toronto, Ontario, Canada

ARTICLE INFO

Article history:
Received 17 June 2016
Received in revised form 2 October 2016
Accepted 16 October 2016
Available online 18 October 2016

Keywords:
Glass polyalkenoate cements
Sternal fixation
Bone cements
Bioactive glass
Tantalum pentoxide
Biocompatibility
Cytotoxicity

ABSTRACT

With over a million median sternotomy surgeries performed worldwide every year, sternal wound complications have posed a serious risk to the affected patients. A rigid therapeutic sternal fixation device has therefore become a necessity. In this work, the incorporation of up to 0.5 mol% of tantalum pentoxide (Ta_2O_5), in exchange for zinc oxide (ZnO), into the SiO_2-ZnO-CaO-SrO-P_2O_5 glass system is presented. The effect of Ta incorporation on the physical, chemical and biological properties of the glass polyalkenoate cements (GPCs) prepared from them have been presented in this manuscript. The data obtained have confirmed that Ta_2O_5 incorporation into the reference glass system results in increased working times, radiopacity, ion solubility, and long-term mechanical stability. The formulated glass systems have also shown clear antibacterial and antifungal activity against both Gram-negative (*Escherichia coli*) and Gram-positive prokaryotes (*Staphylococcus aureus* and *Streptococcus epidermidis*), as well as eukaryotes (*Fusarium solani*). Cytotoxicity testing showed that Ta incorporation results in no toxicity effect and may simulate osseo-integration when tested in animal models. These new metallic-containing biomaterial adhesives have been developed for sternal fixation and repair. As a permanent implant, the formulated adhesives can be used in conjunction with sternal cable ties to offer optimal fixation for patients and reduce post-operative complications such as bacterial infection and pain from micro-motion.

1. Introduction

Glass polyalkenoate cements (GPCs) were developed in the late 1960s. They consist primarily of an organic aqueous solution of polyalkenoic acid (PAA) and an inorganic acid-degradable *fluoro-alumino-silicate* glass [1]. By mixing these constituents together, the glass component degrades to release cations which are responsible for crosslinking the PAA chains to form a polysalt matrix [2]. The acid component facilitates the adhesion of the GPC to bone and plays an instrumental role in controlling the setting reaction and the resultant physical and mechanical properties [1,3].

GPCs have been used in dentistry for over 40 years. They adhere to tooth structure and are both biocompatible and bioactive [4,5]. They do not set with an exotherm nor do they undergo significant volumetric shrinkage with maturation [6]. However, all commercial GPCs contain, and subsequently release, aluminum ions (Al^{3+}) from the glass phase during setting which can have a deleterious effect on the recipient of the cement. To address this issue, attempts have been made to modify the chemistry of the glass phase in order to increase their utility in orthopedic applications [7–9] including vertebroplasty and kyphoplasty [10], arthroplasty [11] and sternal fixation [12,13]. These amendments to the glass reagent can also impart an antibacterial effect to the resultant cements as they mature, due to the release of ions such as zinc (Zn^{2+}) and strontium (Sr^{2+}) [14,15]. Zn is the second most prevalent trace element in the human body and is required for correct functioning of the immune system, healthy bone metabolism, growth and repair, as well as effective wound healing and antibacterial efficacy [16]. Sr plays a physiological role in growth and mineralization of bone tissue [17], therefore up-regulating osteoblastic bone formation. The incorporation of such elements into an Al-free GPC offers the possibility of their slow release at the implant site to facilitate antibacterial and bone regenerating effects.

Tantalum (Ta) is used for orthopedic devices [18–20] due to its excellent physical and biological properties. The Ta ion, itself, is reported to be both bioactive and biocompatible due to the formation of a stable tantalum pentoxide (Ta_2O_5) component on its surface [21,22]. Previous studies [18,23] have shown that Ta surfaces exhibit lower contact angles and higher surface energy than titanium (Ti) or hydroxyapatite (HA) surfaces. Their wettability, high surface energy and enhanced cell-

* Corresponding author at: Department of Mechanical and Industrial Engineering, Faculty of Engineering and Architectural Science, 350 Victoria Street, Toronto M5B 2K3, ON, Canada.
E-mail address: mtowler@ryerson.ca (M.R. Towler).

http://dx.doi.org/10.1016/j.msec.2016.10.024
0928-4931/

material interactions have confirmed that Ta, as a metallic *bio-inert* material, offers a favorable biological environment for adhesion, growth and differentiation of human cells. Further, the incorporation of Ta into acrylic bone cements has been reported to increase radiopacity [24]. Despite some processing challenges [20,25], the inclusion of Ta and other transition metals into ionomer glasses can improve their thermal, optical and chemical stability [26–29].

Median sternotomy surgery is the gold standard for cardiac procedures. Various techniques have been used for sternal fixation, post sternotomy, including wiring [30–32], plate-screw systems [33,34] and cementation [35–37]. All such techniques were critiqued in a review authored by Alhalawani & Towler [12]. Generally speaking, the techniques utilized for sternal fixation have complications restricting their widespread adoption. Sternal wound complications (SWC) occur in 0.4–5% of patients undergoing cardiac surgery, and pose a serious risk to affected patients. In particular, deep SWCs (osteomyelitis and mediastinitis) are associated with a mortality rate between 14 and 47% [33,38,39]. Dehiscence causes up-to 40% mortality and morbidity after median sternotomy with an incidence rate of 0.3–8% [32,40]. The authors previously reported on the potential of Gallium-containing GPCs for sternal fixation [13,41,42]. However, the adhesive properties of the GPCs, deteriorated with increased Ga content, when evaluated in a bovine sternal model [13].

In a previous article [29], the authors synthesized and characterized a wholly new silicate-glass series in which ZnO was substituted with up to 8 mol% Ta_2O_5. In that work, Alhalawani and Towler showed that Ta incorporation into silicate-based glasses was possible by the melt-quenching process. They also confirmed that Ta behaved as a glass former whereas Zn acted as a glass intermediate, depending on its content, in that particular glass system. These novel glasses were designed specifically to formulate a series of GPCs for use in sternal fixation. Initial, unpublished data has confirmed that high Ta-containing glasses (>1 mol% Ta_2O_5) have rheology (long setting and working times) that are deemed unsuitable for sternal applications. Therefore a new series of the previously formulated glass [29] was synthesized containing up to 0.5 mol% Ta_2O_5 and characterized to expand the understanding of this particular bioglass system. The results and conclusions have been reported in part I of this series.

Ta containing GPCs could provide clinicians with an adhesive applicable for sternal fixation and repair. The objective of this work is to characterize the physical, mechanical and biological properties of new adhesive materials based on Ta-containing GPCs, with the intent to optimize these materials for sternal fixation and repair.

2. Materials and methods

2.1. Glass synthesis

Three glasses were prepared for this study, a Ta_2O_5-free SiO_2-ZnO-CaO-SrO-P_2O_5 glass (*TA0*) and two Ta_2O_5-containing glasses (*TA1* and *TA2*) where Ta incrementally replaced ZnO in the *TA0* parent composition (Table 1). Appropriate amounts (Table 1) of analytical grade reagents (Fisher Scientific, Ottawa and Sigma-Aldrich, Oakville, both Canada) were weighed out and mixed into a container. The container was shaken for 15 min and then sieved through a <90 μm mesh. Platinum (Pt.) crucibles and a Lindberg/Blue M model furnace (Lindberg/Blue M, Asheville, NC USA) with a UP550 controller were used for melting the sieved powders (1650 °C, 1.5 h). The melts were shock quenched in water to obtain frit which was then dried in the oven (100 °C, 1 h), ground using a ball mill (400 rounds per minute, 15 min), and sieved once more through a 45 μm mesh. The glass powders resulting were then annealed for 12 h and used for subsequent cement preparation and characterization.

Table 1
Composition of glass series in mole fraction.

	Mol.%		
Oxide	*TA0*	*TA1*	*TA2*
SiO_2	0.48	0.48	0.48
ZnO	**0.36**	**0.358**	**0.355**
CaO	0.06	0.06	0.06
SrO	0.08	0.08	0.08
P_2O_5	0.02	0.02	0.02
Ta_2O_5	–	**0.002**	**0.005**

Bold data indicates significant that Ta_2O_5 was added on the expense of ZnO.

2.2. Cement preparation

Cement samples were prepared by thoroughly mixing the annealed glass (Section 2.1) with poly (acrylic) acid (PAA, Mw, ~213,000 and median particle size <90 μm, Sigma-Aldrich, St. Louis, MI, USA) and distilled water on a glass plate. The cements were formulated in a powder: liquid (P:L) ratio of 1:1, where 1 g of glass was mixed with 0.50 g PAA 200 and 0.50 ml water. Complete mixing was undertaken within 30 s in ambient room temperature (23 ± 1 °C). Cements are subsequently named (*TA0*, *TA1* and *TA2*) after the glasses that they were fabricated from.

2.3. Evaluation of setting characteristics

2.3.1. Working and net setting (hardening) times

The working time of the cements was measured in ambient air (23 ± 1 °C) using a stopwatch, and was defined as the period of time from the start of mixing during which it was possible to manipulate the material without having an adverse effect on its properties. The setting time of cements was measured in accordance with ISO 9917-1:2007 for dental based cements. An empty mould with internal dimensions 10 mm × 8 mm was placed on aluminum foil and filled to a level surface with mixed cement. Sixty seconds after mixing commenced, the entire assembly was placed on a metal block (8 mm × 75 mm × 100 mm) in an oven maintained at 37 °C. Ninety seconds after mixing, a Vicat needle indenter (mass 400 g) was lowered onto the surface of the cement. The needle was allowed to remain on the surface for 5 s, the indent it made was then observed and the process was repeated every 30 s until the needle failed to make a complete circular indent when viewed at ×2 magnification. The net setting time of the three tests was recorded.

2.3.2. Fourier transform infrared (FTIR) spectroscopic study

Three cement cylinders (6 mm high, 4 mm diameter) of each composition were prepared and aged for 1 and 7 days in distilled water. ~0.3 g powdered versions (<90 μm) of each cement were spread onto NaCl crystal discs of 25 mm diameter. Spectra were collected using a Fourier transform infrared spectrometer (Spectrum One FTIR spectrometer, Perkin Elmer Instruments, USA) and background contributions were removed. The sample and the reference background spectra were collected 16 times for each cement formulation in ambient air (23 ± 1 °C). Analysis was performed in the wavenumber ranging from 900 to 3750 cm^{-1} with a spectral resolution of 4 cm^{-1}.

2.4. Evaluation of pH and ion release

2.4.1. Samples preparation

GPC cylinders (6 mm high and 4 mm diameter) were prepared from each glass type for pH testing and ion release studies. Sample solutions were prepared by exposing cylindrical samples ($n = 5$) in calculated quantities (10 ml) of sterile de-ionized (DI) water and incubated (37 °C) for 1, 7 and 30 days.

2.4.2. pH analysis

Changes in the pH of solutions were monitored using a Corning 430 pH meter. Prior to testing, the pH meter was calibrated using pH buffer solution 4.00 ± 0.02 and 7.00 ± 0.02 (Fisher Scientific, Pittsburgh, PA).

2.4.3. Ion release studies

The ion release profile of each specimen was measured using atomic absorption spectroscopy (AAS) on a Perkin-Elmer Analyst 800 (Perkin Elmer, MA, USA). AAS calibration standards for Sr and Zn elements were prepared from a stock solution on a gravimetric basis. Three target calibration standards were prepared for each ion and DI water was used as a control.

2.5. Evaluation of mechanical properties

2.5.1. Determination of compressive strength

The compressive strength (σ_c) of the three GPC compositions were evaluated in ambient air (23 ± 1 °C) according to ISO 9917-1:2007. Cylindrical samples ($n = 5$) were tested after 1, 7 and 30 days ageing (DI water, 37 °C). Testing was undertaken on an Instron Universal Testing Machine (Instron Corp., Massachusetts, USA) using a ±2 kN load cell at a crosshead speed of 1 $mm \cdot min^{-1}$.

2.5.2. Determination of biaxial flexural strength

The biaxial flexural strengths (σ_f) of the cements ($n = 5$) were evaluated using the method as described by Williams et al. [43]. Cement discs were tested, in the wet state, after being aged for 1, 7 and 30 days in distilled water in a 37 °C incubator. Testing was undertaken on an Instron Universal Testing Machine (Instron Corp., Massachusetts, USA) using a ±2 kN load cell at a crosshead speed of 1 $mm \cdot min^{-1}$. The fracture strength was noted for each sample. The load cell error was calculated at 0.005% at 50 N to 0.04% at 100 N, within which these test samples fracture.

2.5.3. Determination of Vickers hardness

Hardness testing was performed on cement discs (2 mm high, 10 mm diameter) with ten measurements taken per disc and three discs used for each glass composition. Samples were tested after 1, 7 and 30 days immersion in sterile DI water at 37 °C. A Shimadzu HMV-2000 μ hardness testing machine (Shimadzu Corporation, Kyoto, Japan) was used. Discs were mounted in epoxy resin and polished using 600 grit silicon carbide polishing paper. Ten Vickers indentations at a load of 500 g and a dwelling time of 15 s were made on each disc. Using the attached light microscope and computer, the diagonals created by the indenter were measured and VHN was calculated using Eq. (1).

$$Hv = 1.854 \frac{F}{d^2} \quad (1)$$

where: F is the applied load (kgf) and d is the diagonal length (mm).

2.6. Evaluation of radiopacity

Cements discs (12 mm diameter, 1 mm thick) were prepared and incubated (37 °C) for 1 h. Once removed from their moulds, the samples were ground using 1200 grit silicon carbide paper until, they were 1 mm thick in accordance with ISO 9917-1:2007 [44]. For the test, the three GPC discs were positioned on dental x-ray film, between an aluminum step wedge (10 steps from thickness from 1.35 mm to 12.62 mm) and an 18 mm thick lead plate. Film was exposed to 70 kV at 7 mA for 0.16 s from the X-ray source (Phot-X II, Belmont Equipment, Somerset, NJ, USA). Optical densities were measured using a QAS Densitometer (Picker International, Highland Heights, OH, USA). Manipulation of results was completed as per the procedure outlined in ISO9917:2007 part 1.

2.7. Antimicrobial analysis

The antimicrobial properties of the cement discs (10 mm in diameter, 2 mm thick, $n = 3$) were evaluated on agar plates, against both prokaryotic and eukaryotic species. Prokaryotic species were one Gram-negative bacterium (*Escherichia coli*) and two Gram-positive bacteria (*Staphylococcus aureus* and *Streptococcus epidermidis*) while the eukaryotic species was a fungus (*Fusarium solani*). Bacterial lawns were spread on Tryptic Soy Agar (3 g/l Tryptic Soy Broth, 15 g/l agar). The antimycotic properties of the discs were assessed on Yeast Malt Agar plates (10 g/l Dextrose, 5 g/l Peptone, 3 g/l Malt Extract, 3 g/l Yeast Extract, 15 g/l agar, pH 8.0). All chemicals were purchased from Fisher Scientific (Ottawa, ON, Canada). Bacterial cultures were grown to an exponential phase (12–16 h), diluted in Physiological Saline Solution (9 g/l NaCl) to 10^6 cells/ml and spread onto TSA. Fungal cultures were grown on YMA for 1 month prior to the experiment, and blocks (1 cm × 1 cm) excised from the outside of the radial colony and transferred to the center of the YMA test plate. Antimicrobial properties were quantified on the bacterial lawns by measuring and comparing the zones of growth inhibition, whereas antimycotic properties against the fungal colonies were compared by measuring the radial growth of the culture.

Samples were sterilized by spreading them in sterile petri dishes and exposing them to ultra violet (UV) light in a biological safety cabinet for 16 h (Bio Klone 2 Series, Class II, Type A2 Biological Safety cabinet, equipped with one integral UV light, Microzone Corporation, Napean, Ontario, Canada).

One disc of each cement (3 discs per plate) was added to each bacterial and fungal plate, evenly spaced on the lawn or around the central fungal colony. Each plate (3 discs per plate) had a single microbial species, and each species was repeated in triplicate for statistical comparisons. The diameters of the inhibition zones, as well as the diameters of the fungal colonies, were measured (mm) and the means and standard deviations of triplicate samples were compared with independent *t*-tests.

2.8. Cytotoxicity testing

Cytotoxicity of the cement discs (10 mm in diameter, 2 mm thick, $n = 3$) was evaluated using chondrocytes for up to 7 days in culture. Cement discs were first sterilized by soaking in 70% ethanol overnight, followed by exposure to UV light for 16 h. Primary bovine articular chondrocytes were then isolated from the metacarpal-phalangeal joints of skeletally mature cattle (12–18 months old) from local slaughter houses by sequential enzymatic digestion. Harvested cartilage slices were incubated in a 0.5% protease (w/v) (Sigma Aldrich Ltd., Oakville, ON, Canada) for 1.5 h at 37 °C followed by 0.15% collagenase A (w/v) (Sigma Aldrich) for 18 h at 37 °C. Chondrocytes were then separated by passing the digest through a 200-mesh filter (Sigma Aldrich). Viable cells (determined by Trypan dye exclusion [45]) were re-suspended in DMEM culture media without phenol red and supplemented with 10% fetal bovine serum and 1% (2 mM) L-glutamine and then seeded on the surface of the cement substrates at a density of 9500 cells per disc. After 1, 3 and 7 days of culture, cell viability was assed using a Methyl Tetrazolium (MTT) assay kit (Sigma Aldrich) according to the manufacturer's instructions. As the presence of the cement discs would interfere with the absorbance measurements, aliquots of the precipitate solution (without cells) were analyzed separately. All results were compared to control cultures of the same number of cells seeded directly onto tissue culture plastic.

2.9. Ex-vivo bond strength testing

Samples cut from femur cortical bone and reduced to cylindrical bone samples were utilized to study the ability of the developed materials to adhere to bovine cortical bone. Bone samples were machined to their final geometries using a computer numerical control (CNC) machine (Fig. 1). The dimension of the samples is measured accurately using a clipper. Fresh bone samples shortly after machining were sterilized and then kept in a protector tube at −4 °C. Prior to testing, the

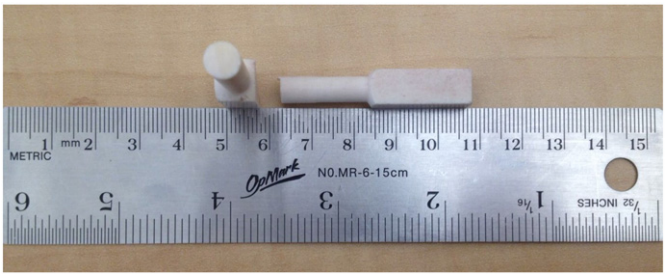

Fig. 1. Cross-sectional view (left) and side view (right) of the bovine cortical bone sample used for *ex-vivo* adhesion testing.

samples were left for 0.5 h at ambient temperature before applying the adhesive. The adhesive of each material (*TA0*, *TA1* and *TA2*) was prepared as discussed in Section 2.2 and applied directly on both sides of the bovine bone ($n = 3$). Each sample was held together for one minute to allow for attachment before it was placed in DI water and incubated (37 °C, 1 day) prior to testing. Testing was undertaken on an Instron Universal Testing Machine (Instron Corp., Massachusetts, USA) using a ± 2 kN load cell at a crosshead speed of 1 mm·min^{-1}. The fracture strength (N) was noted for each sample.

2.10. Statistical analysis

Non-parametric Kruskal-Wallis H Test was used to analyze the data. Mann-Whitney *U* test was used to compare the relative means and to report the statistically significant differences when $P \leq 0.05$. Statistical analysis was performed on all groups where $n \geq 3$. Statistical analysis was performed using SPSS software (IBM SPSS statistics 21, IBM Corp., Armonk, NY, USA).

3. Results and discussion

3.1. Evaluation of cement setting characteristics

3.1.1. Working and net setting times

The working and setting times of the cement series were evaluated with respect to the increasing concentration of Ta_2O_5 in the glass phase, and are presented in Fig. 2. Working times were recorded as 40, 48 and 63 s for *TA0*, *TA1* and *TA2*, respectively (Fig. 2a). There is a statistical significant difference ($P = 0.008$) among all groups. The setting times are also recorded (Fig. 2b). The Ta_2O_5-free GPCs (*TA0*) presented a setting time of 197 s which decreased significantly ($P = 0.007$) to 156 s for *TA1* and then increased significantly ($P = 0.008$) to 202 s for *TA2*. There is no information on the setting chemistry of Ta-containing GPCs in the literature that can be referenced for comparative purposes. Working and setting times were dependent on the concentration of Ta_2O_5 incorporated into the glass. The workability of *TA0* and *TA1* cements is too short to be considered suitable for sternal fixation application. *TA2*, however, is more suitable for clinical use due to its longer working and setting times, when compared to those of Ta-free cements. The setting time of all cement formulations lies within the limits outlined by ISO9917-1:2007 for dental based materials/cements, where a minimum of 90 s and a maximum of 360 s is required [44]. The setting and working times of Ta-containing cements can be extended/shortened, by changing the powder (glass):liquid (acid + PAA) ratios and/or by slightly increasing the Ta content within the glass matrix, to meet the requirements of orthopedic surgeries such as sternal fixation. Pre-clinical feedback from cardiac surgeons has confirmed that the incorporation of Ta (up to 0.5 mol%) has resulted in adhesive materials suitable for sternal fixation. Ta^{5+} acts as a network former by adopting six-fold coordination (TaO_6). Zn however may either adopt four-fold coordination in oxygen polyhedron and act as a network former, or adopt six-fold coordination and act as a network modifier [29]. Substituting Ta^{5+} with Zn^{2+} is expected to result in a better glass structure in terms of stability and electro-neutrality. Ta^{5+} provides a larger number of positive charges when compared to Zn^{2+} and therefore acts as a charge-efficient network former. This results in a delay in the gelation process between the COOH groups and Ta^{5+} ions resulting in longer handling times. The un-expected decrease in the T_s of *TA1* can be attributed to the glass particle size, or to slight changes in the glass compositions. The cements with the highest amounts of Ta_2O_5 (*TA2*) exhibited longer working times and similar setting times than the Ta_2O_5-free GPCs and are preferable when compared to *TA0* and *TA1*, as clinical materials.

3.1.2. FTIR spectroscopic study

FTIR can provide characteristic information on the setting kinetics of GPCs. FTIR transmittance spectra of the cement series, obtained at days 1 and 7, post cement preparation and maturation in DI water, are shown in Fig. 3 in the range 3750–900 cm^{-1}. The obtained bands are centered at 3254, 1555, 1455, 1408, 1320, 1083, and 965 cm^{-1}. Table 2 shows a complete list of the obtained vibration frequencies and their assignments. The broad peak centered at 3254 cm^{-1} was observed for all spectra and is assigned to the O—H stretch of adsorbed/embedded water within the poly-salt matrix. This O—H peak broadens at 7 days, particularly for *TA0* and *TA1*. However, the peak intensity does not change significantly for *TA2* indicating that *TA2* retains the absorbed water for longer times, when compared to *TA0* and *TA1*. This results from the former role of Ta in these materials and indicates that the gelation/hardening reactions within *TA2* are longer, resulting in longer setting times. The peaks centered at 1555, 1455, 1408 and 1320 cm^{-1} are assigned to the asymmetric/symmetric stretching vibrations of the carboxyl COO, which could be assumed to be an asymmetrically/

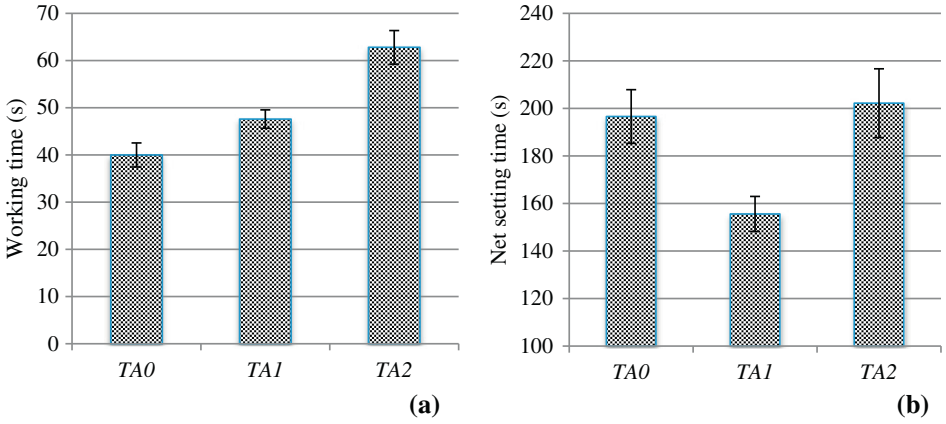

Fig. 2. Working and setting times for Ta-containing silica based GPCs. Error bars represent standard deviation from the mean ($n = 5$).

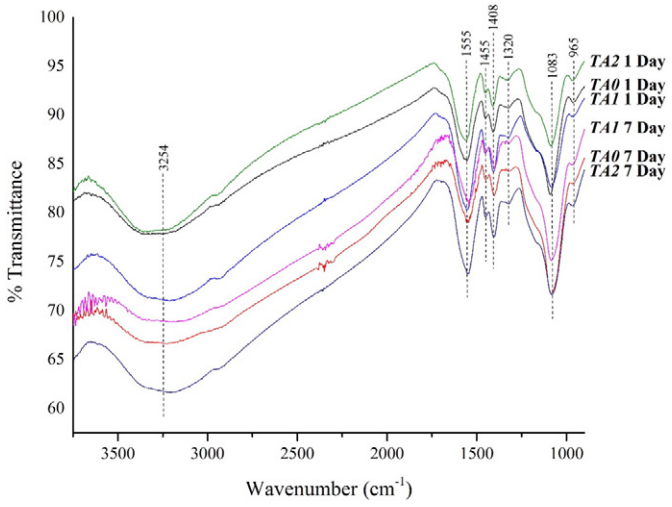

Fig. 3. FTIR spectrum of cement series over 1 and 7 day, post cement preparation and ageing in DI water.

symmetrically bonded COO–X molecule, where X represents a possible metal cation. Both COO-Ca^{2+} and COO-Sr^{2+} groups were identified within the range 1630–1540 cm^{-1} [46] and within the range 1490–1460 cm^{-1} [47]. Small shifts to lower wavenumber/frequency were observed for the transmittance bands at 1555, 1455, 1408 and 1320 cm^{-1} with time. This small shift is caused by the increase in cross-linking (bonding) between the dissociated COO– group and metal cations, such as the Ca^{2+}, Sr^{2+} and Zn^{2+}, to form a metal carboxylate in the cements. Alternatively, the small shifts in frequency of these bands can confirm the complexation of glass cations to the COOH and the consequent changes within the glass structure, resulting from the insertion of Ta_2O_5 within the glass network. This is in good agreement with the literature [13,48–50] [51] which also confirms that the 1083 cm^{-1} peak represents the Si—O—Si bridges of the cements and as such its relative increase or decrease in intensity correlates to an increase or decrease in the formation of bridging oxygens. The peak at 1083 cm^{-1} could also represent the Si—O—Ta bridges within the glass structure. The peak at 965 cm^{-1} is assigned to the Si—OH bridges within the glass network. The peaks obtained from samples matured for 1 and 7 day samples do not show a trend in relation to the Ta_2O_5 content, however the *TA2* peak was observed at the highest %transmittance (83%t) for 1 day samples. This could possibly be due to the changes within the glass network in relation to the insertion of Ta_2O_5 metallic ions into the silicate network, hence disrupting the network and resulting in longer setting times. *TA2* experiences a drop in %transmittance for the 7 day sample (65%t) and this may be attributed to the formation of stronger bonds between the glass cations and acidic anions during maturation in DI water indicating that *TA2* results in stronger cements upon immersion in a medium such as DI water.

Table 2
Characteristic vibration frequencies (cm^{-1}) in FTIR spectra of the cement series.

Infrared band position (cm^{-1})	Peak assignment	Ref.
3254	O—H stretching	[13,52]
1555–1320	Asymmetrical COO–X bonding, where X represents a possible metal cation (Ca^{2+}, Sr^{2+}, Zn^{2+})	[13]
1083	Si—O—Si/Si—O—Ta stretching vibration	[51]
965	Si—OH deformation vibration	[51]

3.2. pH and ion release studies

3.2.1. pH analysis

The changing pH values of the DI water (pH = 6.0) as a function of Ta_2O_5 content are plotted in Fig. 4. Comparing *TA0* with *TA2*, there was a significant increase in pH (~6.0–6.6, $P = 0.008$) for 1 day samples, a significant decrease in pH (~6.9–6.6, $P = 0.008$) for 7 day samples and almost identical pH values (~6.82, $P = 0.310$) for 30 day samples. Further, there was a statistically significant difference ($P < 0.05$) in the pH values when comparing *TA0* and *TA1* for 1 day ($P = 0.032$) and 30 day ($P = 0.016$) groups. However, there was no significant difference ($P = 0.421$) between *TA0* and *TA1* for 7 day samples. The pH was dependent on immersion time with values varying between ~6 and ~6.9 for all cement formulations. However, it is important to note that slight or no change in pH values ($P > 0.05$) were obtained when comparing 7 and 30 days samples for all cement formulations.

When a GPC sample is aged in DI water, hydrogen ions diffuse and dissociate the polycarboxylic chains within the GPC structure and prompt the glass particles to release cations into the environment. This process is controlled by the concentration of hydrogen ions in both the immediate environment (DI water) and the GPC matrix (COOH groups) [53]. In this study, *TA2* exhibited the longest working and setting times of the three cement compositions. This resulted in higher pH values, when compared to *TA0* and *TA1*. The decrease in the pH of *TA2* samples at day 7, when compared to that of *TA1*, indicates that the incorporation of Ta_2O_5 facilitates the formation of a stronger network during ageing. Further, identical pH for *TA0* and *TA2* at day 30 shows that the incorporation of Ta_2O_5 at the expense of ZnO does not 'negatively' affect the setting reaction.

3.2.2. Ion release profiles

The changing ion release profiles for Zn^{2+} and Sr^{2+} ions as a function of maturation are plotted in Fig. 5. Statistical analysis was performed with respect to Ta_2O_5 content (Table 3). This study considers the release of Zn^{2+} and Sr^{2+} only due to their content in the precursor glasses and their therapeutic importance in the clinical field. The release of Zn^{2+} decreased with Ta_2O_5 content (Fig. 5a) and was also dependent on immersion time. This was expected as Ta_2O_5 was substituted with ZnO in *TA1* and *TA2*. Fig. 5b represents the release of Sr^{2+} ions with both Ta_2O_5 content and maturation, peaking at ~11.7 ppm for *TA2* cements after 30 days of immersion. Again, this is attributed to the longer setting reaction of *TA2* cements, which retards initial cross-linking after the attack of the PAA on the glass structure. This phenomenon can also be attributed to the slow reaction of the Ta^{5+} ions with the carboxylic groups.

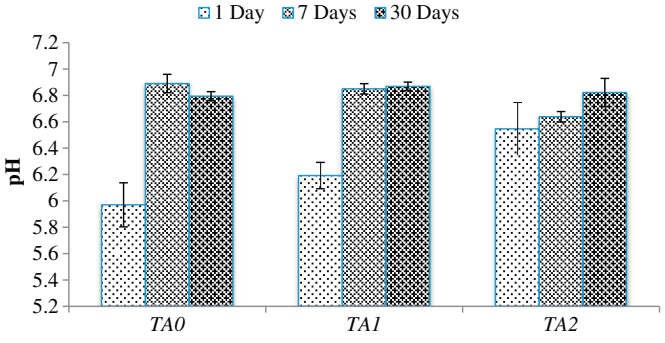

Fig. 4. pH measurements during cement solubility in DI water for 1, 7 and 30 days, post cement preparation. Error bars represent standard deviation from the mean ($n = 5$).

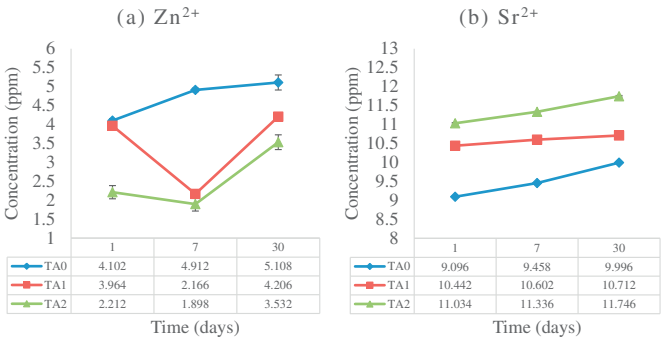

Fig. 5. Release profiles of (a) Zn^{2+} and (b) Sr^{2+} ions during cement ageing in DI water. Error bars represent standard deviation from the mean ($n = 5$).

3.3. Evaluation of mechanical properties

3.3.1. Determination of compressive and biaxial flexural strengths

Compressive (σ_c) and biaxial flexural (σ_f) strength results of the cement series tested over 1, 7 and 30 days are presented in Fig. 6. The highest σ_c and σ_f are 21 MPa and 22 MPa, respectively and are obtained for *TA1* after 7 days maturation. *TA1* had the shortest setting time (Fig. 2b) and is assumed to have higher strength resulting from the quicker cation-anion reactions within the matrix. However this behavior was only noted for 7 day results. There was no significant difference ($P > 0.05$) in σ_c with respect to either maturation or Ta_2O_5 content among the groups. σ_f, however, showed variation with respect to both Ta content and maturation. With respect to Ta_2O_5 content, there was a significant increase in the σ_f ($P = 0.008$) increasing from 16 (*TA0*) to 21 MPa (*TA2*), when tested at day 30. With respect to ageing, the σ_f of a) *TA0* decreased significantly ($P = 0.005$) from 21 (day 1) to 16 MPa (day 30), b) *TA1* increased significantly ($P = 0.035$) from 18 (day 1) to 21 MPa (day 30) and c) *TA2* increased with no statistical significance ($P = 0.062$) from 19 (1 day) to 21 MPa (30 days). The incorporation of Ta has a long-term effect on σ_f of the cements prepared from them. This can be attributed to 1) the slow reactions between Ta and the PAA chains as Ta is impervious to acid attack, 2) the dissolution of the glass particles, *i.e.* Ta increases the dissolution of the glass particles within the cement matrix resulting in the release of ions that further crosslink PAA chains [54].

3.3.2. Determination of Vickers hardness

The Vickers hardness of the cement series is shown in Fig. 7. Hardness varied with Ta_2O_5 content and exhibited a similar trend to the compressive and biaxial flexural strength results. Hardness of *TA0* decreased with maturation, from 14 to 9 HV. Hardness of *TA1* and *TA2* however, increased with maturation from 11 to 18 HV and from 13 to 18 HV, respectively. The incorporation of Ta_2O_5 presented higher hardness values and exhibited a significant increase during cement maturation. Statistical significant differences were observed for *TA0 versus TA1* for 30 day samples ($P = 0.008$) and for *TA0 versus TA2* for 7 and 30 day samples ($P < 0.05$). There is no difference among the *TA1* and *TA2* groups.

Table 3
Means comparison of Zn^{2+} and Sr^{2+} ion release with respect of Ta_2O_5 content.

	Groups	1 day	7 day	30 day
Zn ion release	*TA0 versus TA1*	0.690	0.008*	0.310
	TA0 versus TA2	0.032*	0.008*	0.095
	TA1 versus TA2	0.008*	0.222	0.151
Sr ion release	*TA0 versus TA1*	0.008*	0.008*	0.032*
	TA0 versus TA2	0.008*	0.008*	0.008*
	TA1 versus TA2	0.008*	0.008*	0.008*

* Significant at $P \le 0.05$.

These results follow the same trend as those of the σ_f, therefore the σ_f discussions, provided earlier, may hold true for the hardness results.

3.4. Evaluation of radiopacity

Radiopacity results are shown in Fig. 8. All cements exhibited radiopacity higher than that of Al (280%, 290% and 300% of that of Al for *TA0*, *TA1* and *TA2*, respectively). *TA2* was the most radiopaque cement tested while the Ta_2O_5-free cement (*TA0*) had a similar radiopacity ($P > 0.05$), when compared to that of *TA2*. The materials developed in this study are more radiopaque than the Zn-GPCs previously produced by the authors [10]. The high radiopacity of Zn-based cements was previously attributed to both the ZnO and SrO content [55,56]. Here, it can be seen that replacing the ZnO with the Ta_2O_5 has increased radiopacity, presumably because Ta_2O_5 (8.2 g/cm^3) is more radiopaque than ZnO (5.61 g/cm^3) [57]. Increased radiopacity allows for easier subcutaneous monitoring of the implant.

3.5. Antimicrobial evaluation

The antimicrobial properties of Ta-containing GPCs were assessed against both Gram-negative and Gram-positive prokaryotes (Fig. 9), as well as eukaryotes (Fig. 10). All GPCs exhibited a level of both antibiotic and antimycotic activity within these experimental parameters.

Within the GPCs assessed in this study, ZnO was substituted with Ta_2O_5 (increasingly in *TA0*, *TA1* and *TA2*; see Table 1 and Fig. 5), and lower levels of antimicrobial activity were thus predicted, since the Zn ion is renowned for its antibiotic effect, whereas Ta is considered less bio-toxic [20,58]. However, the inhibition effect was comparable ($P > 0.05$) with respect to increasing Ta_2O_5 content for all bacterial species under study. Similar inhibition zones (8–9 mm ± 0.4) were obtained for one Gram-positive (*S. aureus*) and one Gram-negative (*E. coli*) strain, while a second Gram-positive bacterium (*S. epidermidis*) was even more susceptible to ion release by the GPCs, with an inhibition zone almost twice as large as the first two strains (15 mm ± 0.6). This species-dependent activity is in agreement with the literature [59], which indicated that factors influencing bacterial proliferation on a material surface are dependent on both the properties of the surface and the bacterial strain, particularly with regards to cell wall composition. It was reported by Wren et al. [60] that Zn^{2+} is particularly inhibitory against *E. coli*, and was thus the ion of interest in this study. However, as mentioned above, increasing levels of Ta_2O_5, accompanied by decreasing levels of ZnO, did not demonstrate any observable influence on the antibacterial properties of the GPCs against any of the bacterial strains of interest. The uniform antibacterial effect of the materials under study could be attributed to 2 properties:

(1) The increased release of Sr (see Fig. 5) with the increased amount of Ta_2O_5 (and decreasing amounts of ZnO), and/or
(2) The increased wettability of the surface of Ta-containing materials, when compared to Ta-free GPCs (this will be a subject of further research).

Sr is another ion with reported antimicrobial impact [61] and, although incorporated into the GPCs at the same level in *TA0*, *TA1* and *TA2*, it is released at increasing levels with higher Ta_2O_5 levels due to structural changes in the glass. Thus, the increasing antimicrobial activity of Sr could offset the decreasing antimicrobial activity of Zn, with the increased incorporation of Ta in the GPCs. It was reported that Ta surfaces result in lower contact angles, higher surface energy and improved antibacterial effect when compared to Ti or HA surfaces, and thus Ta itself could have indirect antimicrobial effects too [18,22,23].

During ageing, the antibacterial effect exhibited by these cements was expected to decrease as a result of the continuous cross-linking within the matrix [13], and due to potential time- and morphology-

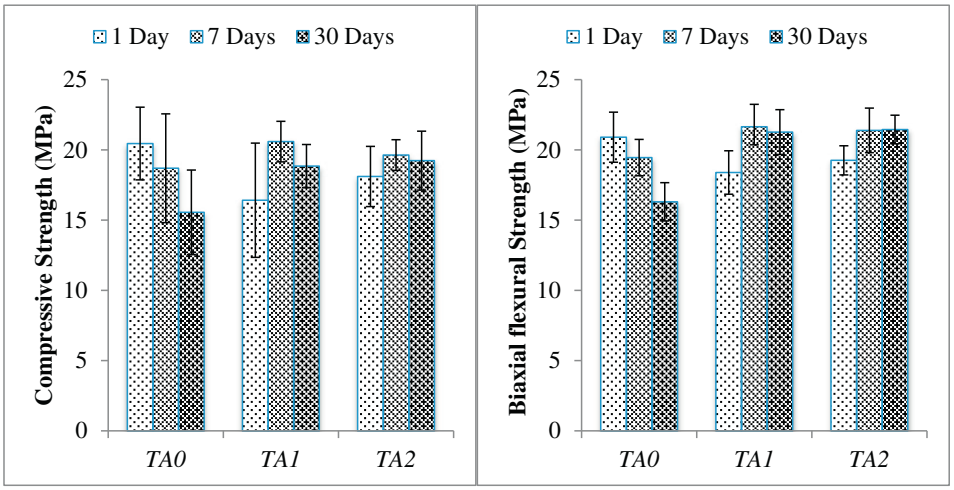

Fig. 6. Compressive (a) and biaxial flexural (b) strengths of the cement series when aged in DI water for 1, 7 and 30 days. Error bars represent standard deviation from the mean ($n = 5$).

dependent adaptation of microbial species [62,63]. However the materials under study have shown that the initial antibacterial effect, presumably from ions leached into the agar, persisted for up to 30 days with no significant change ($P > 0.05$) when compared to day 1. The release of ions into a liquid medium could significantly affect such time studies, and is an interesting potential follow-up study, particularly the antimicrobial effects of these ions in saturated biofilms, which are so relevant in nosocomial environments [62].

A single fungal eukaryotic strain, *Fusarium solani*, was chosen to explore the antimycotic properties of the GPCs and the results are presented in Fig. 10. A control square fungal colony (3.6 × 7.2 mm; sourced from the edges of a week-old colony) was transferred onto an agar plate, and its growth monitored over a period of 30 days. At day 1 (Fig. 10a), the hyphal colony started to grow outward (14.4 × 8.6 mm). At day 7 (Fig. 10c), the control colony exhibited circular flat shape with a diameter of 52 mm. At day 30 (Fig. 10e), the control colony had extended prolifically to a diameter of 73 mm. Similarly, a flat square inoculum block (3.6 × 7.2 mm) was tested, with the cement substrates (*TA0*, *TA1* and *TA2*) placed on the surface of the agar plate at equal distances from the central colony. At day 1, day 7 and day 30 (Fig. 10b, d and f), fungal growth and colony morphology was clearly influenced by exposure to the GPCs, as compared to the control. At day 7 (Fig. 10d), the colony was confined to the center of the plate, growing upward in a raised circular shape, morphologically distinct from the control, with a diameter of 12.5 mm, approximately 20% of the diameter of the control at day 7. At day 30 (Fig. 10f), colony morphology was similarly influenced by the presence of the GPCs, constrained at 10.6, 2.5 and 4.6 mm away from the center of *TA0*, *TA1* and *TA2*, respectively. According to the authors' knowledge, until now, no detailed studies assess the antifungal performance of GPCs or Ta-containing GPCs. It is clear from the results obtained that the formulated GPCs have antifungal properties. Unlike the antibiotic properties of these GPCs, according to these preliminary studies, the antifungal properties were shown to (1) decrease with increasing Ta content (and increasing Zn content), and (2) decrease with maturation. This behavior is attributed to decreasing the Zn content (Fig. 5) and to the decreasing release of ions with ageing. However, after *in-vivo* placement of GPCs, any decreasing antimicrobial properties with age should accompany an improvement in immune response/reaction with the healing process, since the skin itself acts as a physical antibiotic barrier during the healing process [64]. Thus the initial antimicrobial activity is of greatest interest. In contrast to the antibacterial observations, increased release of Sr, associated with increasing the Ta content, did not compensate for the decreased release of Zn^{2+}, therefore Sr^{2+} is not as antifungal as Zn^{2+}. Despite some variation, it can be seen that the formulated cement substrates have clear antibacterial and antifungal activity, as evaluated on solid media, suggesting that the substrates are promising candidates to further test long-term, liquid and *in-vivo* antimicrobial properties.

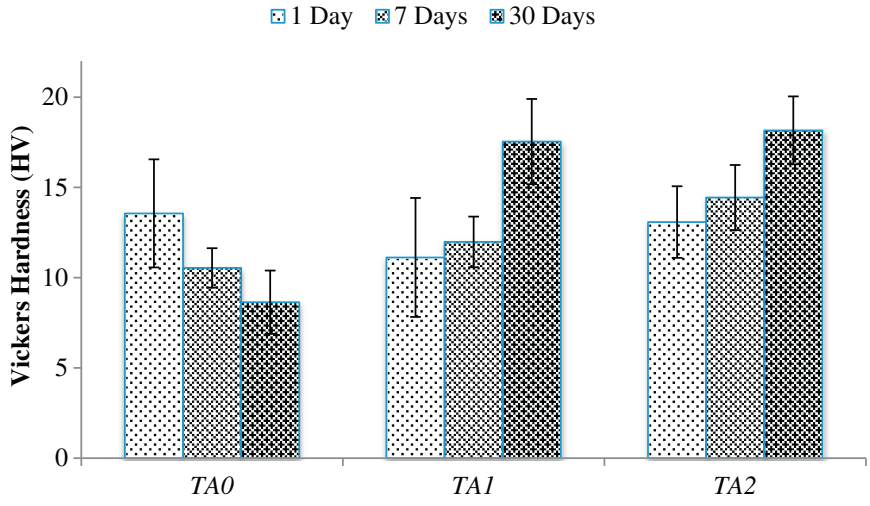

Fig. 7. Vickers hardness of the cements when matured for 1, 7 and 30 days, post cement preparation. Error bars represent standard deviation from the mean ($n = 5$).

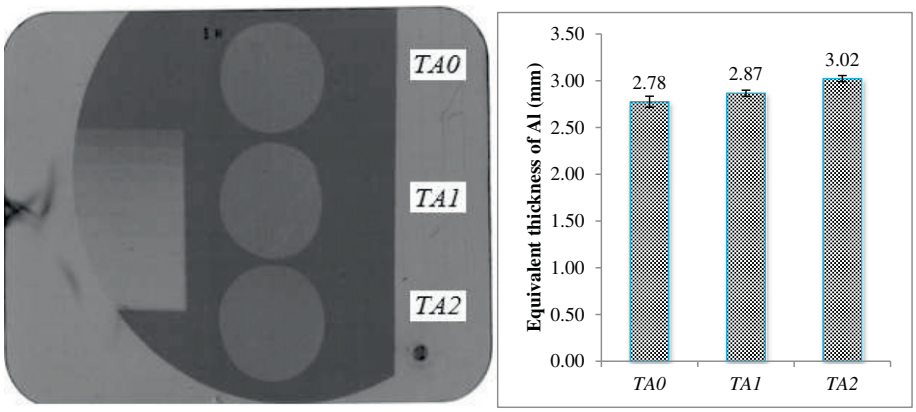

Fig. 8. (a) Radiographic images of cement discs and the aluminum step wedge. (b) The radiopacity of the discs recorded in mm Al. Error bars represent standard deviation from the mean ($n = 5$).

3.6. Cytotoxicity testing

Fig. 11 shows the cell viability results of each of the materials tested after 1, 3 and 7 days of culture, compared to chondrocytes seeded on tissue culture plastic (*Control*). All cements tested did not appear to display any cytotoxic effects as cells appeared to proliferate when cultured on the material surfaces. Cell viability on the *TA0* surfaces changed little ($P > 0.05$) with culture time reducing from 191% of control (day 1) to 176% (day 7). This behavior could be attributed to the ion release products from the cement. Immediately after cell seeding and during the first 24 h of culture, the cement releases some of its 'unbound' cations at different rates [65]. The release of Si, Sr, Ca, P and Sr ions would be expected to stimulate biological responses such as cell attachment and proliferation [66]. *TA1* cements were similar with cell viability ranging between 221% and 349% with no apparent influence of culture time ($P > 0.05$). *TA2* cements performed differently

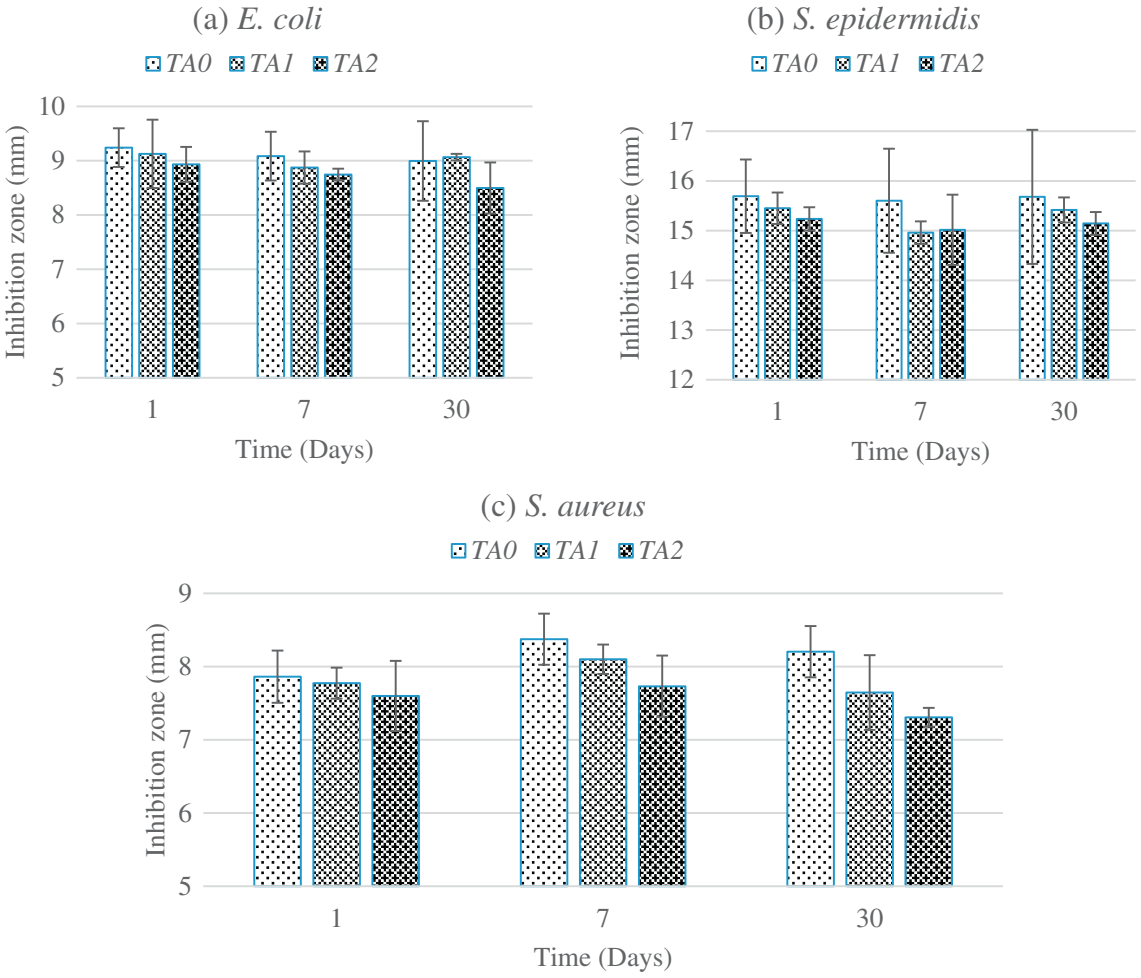

Fig. 9. Inhibition zones of a) *E. coli*, b) *S. epidermidis* and c) *S. aureus* lawns on agar media, in response to *TA0*, *TA1* and *TA2*, evaluated after 1, 7 and 30 days maturation and incubated at 37 °C. Error bars represent standard deviation from the mean ($n = 3$).

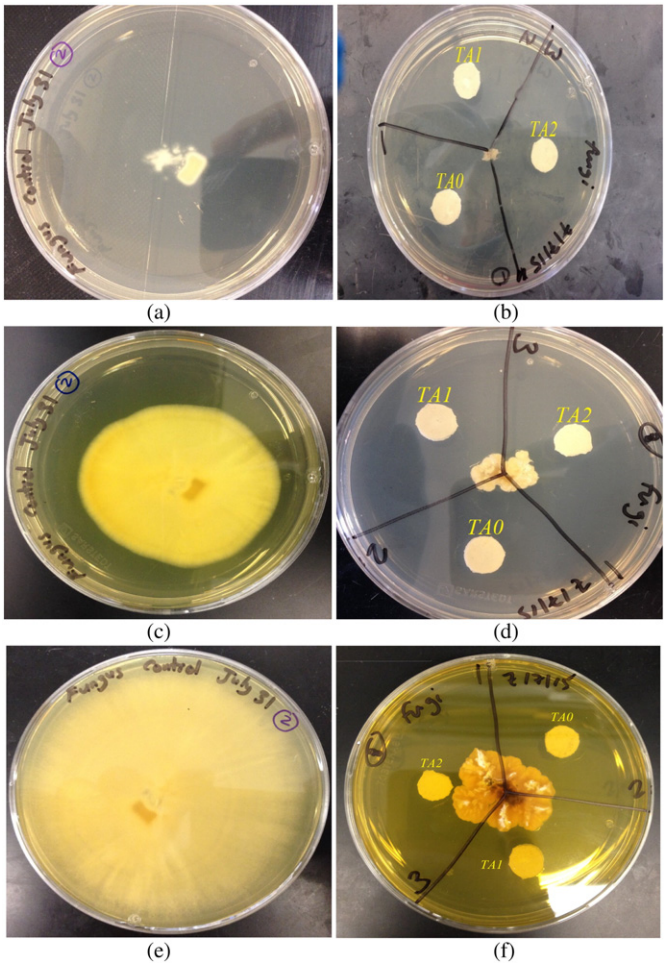

Fig. 10. Colony morphology of *Fusarium solani* fungus aged with no samples (control) and tested with *TA0*, *TA1* and *TA2* over a period of 1 (a and b), 7 (c and d) and 30 days (e and f), respectively.

than the other cements with cell viability ranging between 174 and 220% (day 1–3) and then increasing to 760% (day 7). The substitution of Ta_2O_5 for ZnO may be responsible for the observed proliferative effect. Cell attachment and proliferation are primarily associated with a material's surface properties such as wettability and the material's bulk/volume composition [20]. An *in-vitro* study has shown that human osteoblast cells exposed to Ta and HA coatings exhibit equally excellent cellular adherence and viability [23] due to the lower contact angles and higher surface energy of Ta when compared to Ti or HA surfaces [18,23]. Therefore, Ta incorporation into bioactive glasses may not only stimulate osseo-integration but also their cell-material interactions and long-term mechanical stability. This is supported by a previous *in-vivo* study of bioactive glass coatings on Ti plates which resulted in enhanced initial tissue attachment, bone growth and rapid osseo-integration [67].

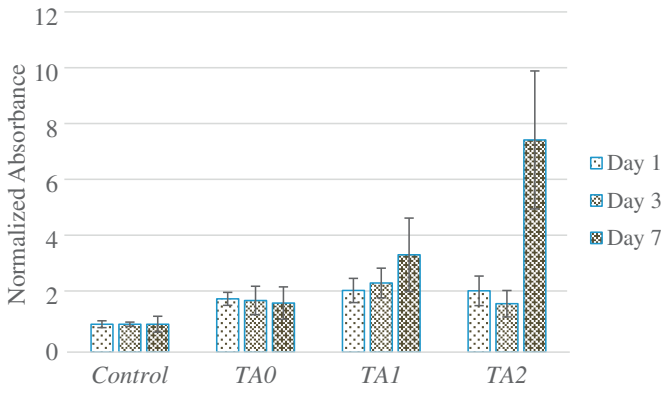

Fig. 11. Cell viability results of the *Control* fibroblast cells and the formulated cements over 1, 3 and 7 days, post cement preparation and incubation. Error bars represent standard deviation from the mean ($n = 3$).

3.7. Ex-vivo bond strength testing

This study considers a preliminary adhesion test to evaluate the bond strength of the adhesive materials, when applied to bovine femoral cortical bone. Fig. 12 shows the tensile strength results obtained at day 1, post sample preparation and incubation. It is obvious that *TA0* has the highest strength (1.6 MPa). However comparable results ($P > 0.05$) were obtained for *TA1* (1.1 MPa) and *TA2* (1.0 MPa) samples. Further studies with a larger number of samples tested over a longer ageing period may reveal statistically significant differences.

The adhesion and tissue bonding of sternal fixation devices are crucial for satisfactory performance. The results of this preliminary study confirm the mechanical testing results obtained in Section 3.3. Generally, it can be observed that Ta-free cements result in slightly higher, but comparable, strength values at day 1. Comparable results are attributed to the little change in the former glass materials (Table 1). This means that further incorporation of Ta into GPCs may have unfavorable effect on their early strength values resulting from the slow reactivity of Ta with PAA. As pointed earlier, Ta is impervious to acid attack at the early stage of the reaction, therefore affecting the cation-anion chelating reactions. This however changes during cement ageing allowing for improved adhesion and mechanical stability.

4. Conclusions

The results reported here confirm that cements based on the tantalum-containing glass have rheology, strength, radiopacity, antibacterial and *in-vitro* behavior suitable for sternal fixation. This study has also confirmed the ability of the formulated materials to adhere to bovine femoral bone. As a permanent implant, the formulated adhesives can be used in conjunction with sternal cable ties to offer optimal fixation and reduce post-operative complications such as bacterial infections and pain from sternal displacement. Further research will involve *in-vivo* testing of the propriety material utilizing animals and cadaver sterna.

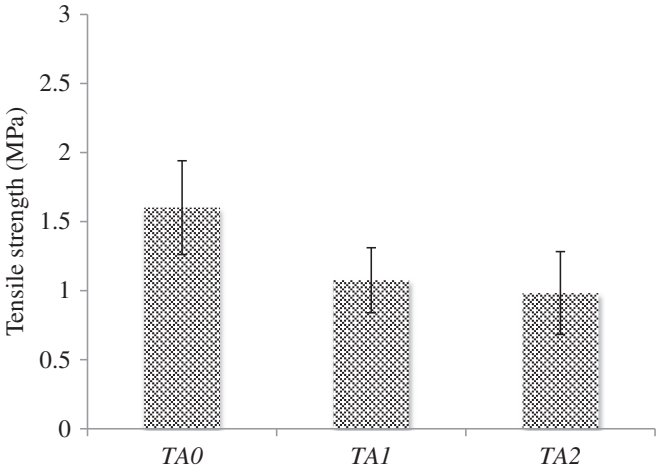

Fig. 12. Mechanical testing results of the bovine femur cortical bones adhered using the formulated cements and aged in DI water for 1 day at 37 °C. Error bars represent standard deviation from the mean ($n = 3$).

Acknowledgment

The authors gratefully acknowledge the financial assistance of the Collaborative Health Research Project, CIHR/NSERC (315694-DAN). The authors are also thankful to Dr. Declan Curran (Medtronic, Ireland) for his advice, Dr. Daniel Boyd (Dalhousie University, Canada) for his assistance with radiopacity testing, Dr. Ahmad Varvani for the bone sample design and Mr. Chao Ma for machining the samples (both Ryerson University).

References

[1] J.W. Nicholson, Adhesive dental materials—a review, Int. J. Adhes. Adhes. 18 (1998) 229–236, http://dx.doi.org/10.1016/S0143-7496(98)00027-X.
[2] J.W. Nicholson, Chemistry of glass-ionomer cements: a review, Biomaterials 19 (1998) 485–494.
[3] A.M.F. Alhalawani, D.J. Curran, D. Boyd, M.R. Towler, The role of poly(acrylic acid) in conventional glass polyalkenoate cements: a review, J. Polym. Eng. 36 (3) (2016) 221–237.
[4] A.O. Akinmade, J.W. Nicholson, Glass-ionomer cements as adhesives, J. Mater. Sci. Mater. Med. 4 (1993) 95–101.
[5] J.F. McCabe, D. Watts, H.J. Wilson, H.V. Worthington, An investigation of test-house variability in the mechanical testing of dental materials, J. Dent. 18 (1990) 90–97.
[6] D. Boyd, M.R. Towler, A.W. Wren, O.M. Clarkin, D.A. Tanner, TEM analysis of apatite surface layers observed on zinc based glass polyalkenoate cements, J. Mater. Sci. 43 (2008) 1170–1173, http://dx.doi.org/10.1007/s10853-007-2362-7.
[7] M. Navarro, A. Michiardi, O. Castaño, J.A. Planell, Biomaterials in orthopaedics, J. R. Soc. Interface 5 (2008) 1137–1158, http://dx.doi.org/10.1098/rsif.2008.0151.
[8] D. Boyd, O.M. Clarkin, A.W. Wren, M.R. Towler, Zinc-based glass polyalkenoate cements with improved setting times and mechanical properties, Acta Biomater. 4 (2008) 425–431, http://dx.doi.org/10.1016/j.actbio.2007.07.010.
[9] T.M. Eidem, A. Coughlan, M.R. Towler, P.M. Dunman, A.W. Wren, Drug-eluting cements for hard tissue repair: a comparative study using vancomycin and RNPA1000 to inhibit growth of *Staphylococcus aureus*, J. Biomater. Appl. 28 (2014) 1235–1246, http://dx.doi.org/10.1177/0885328213503388.
[10] G. Lewis, M.R. Towler, D. Boyd, M.J. German, A.W. Wren, O.M. Clarkin, et al., Evaluation of two novel aluminum-free, zinc-based glass polyalkenoate cements as alternatives to PMMA bone cement for use in vertebroplasty and balloon kyphoplasty, J. Mater. Sci. Mater. Med. 21 (2010) 59–66, http://dx.doi.org/10.1007/s10856-009-3845-7.
[11] O.M. Clarkin, D. Boyd, S. Madigan, M.R. Towler, Comparison of an experimental bone cement with a commercial control, Hydroset, J. Mater. Sci. Mater. Med. 20 (2009) 1563–1570, http://dx.doi.org/10.1007/s10856-009-3701-9.
[12] A.M.F. Alhalawani, M.R. Towler, A review of sternal closure techniques, J. Biomater. Appl. 28 (2013) 483–497 (http://www.ncbi.nlm.nih.gov/pubmed/23812580).
[13] A.M.F. Alhalawani, D. Curran, B. Pingguan-Murphy, D. Boyd, M. Towler, A novel glass polyalkenoate cement for fixation and stabilisation of the ribcage, post sternotomy surgery: an ex-vivo study, J. Funct. Biomater. 4 (2013) 329–357http://www.mdpi.com/2079-4983/4/4/329/.
[14] M. Darling, R. Hill, Novel polyalkenoate (glass-ionomer) dental cements based on zinc silicate glasses, Biomaterials 15 (1994) 299–306 http://dx.doi.org/10.1016/0142-9612(94)90055-.
[15] M.R. Towler, S. Kenny, D. Boyd, T. Pembroke, M. Buggy, R.G. Hill, Zinc ion release from novel hard tissue biomaterials, Biomed. Mater. Eng. 14 (2004) 565–572.
[16] R.B. Saper, R. Rash, Zinc: an essential micronutrient, Am. Fam. Physician 79 (2009) 768–772.
[17] P.J. Marie, P. Ammann, G. Boivin, C. Rey, Mechanisms of action and therapeutic potential of strontium in bone, Calcif. Tissue Int. 69 (2001) 121–129.
[18] V.K. Balla, S. Bodhak, S. Bose, A. Bandyopadhyay, Porous tantalum structures for bone implants: fabrication, mechanical and in vitro biological properties, Acta Biomater. 6 (2010) 3349–3359, http://dx.doi.org/10.1016/j.actbio.2010.01.046.
[19] K.B. Sagomonyants, M. Hakim-Zargar, A. Jhaveri, M.S. Aronow, G. Gronowicz, Porous tantalum stimulates the proliferation and osteogenesis of osteoblasts from elderly female patients, J. Orthop. Res. 29 (2011) 609–616, http://dx.doi.org/10.1002/jor.21251.
[20] V.K. Balla, S. Bose, N.M. Davies, A. Bandyopadhyay, Tantalum—a bioactive metal for implants, JOM 62 (2010) 61–64, http://dx.doi.org/10.1007/s11837-010-0110-y.
[21] T. Miyaza, H.-M. Kim, T. Kokubo, C. Ohtsuki, H. Kato, T. Nakamura, Mechanism of bonelike apatite formation on bioactive tantalum metal in a simulated body fluid, Biomaterials 23 (2002) 827–832.
[22] Y.-Y. Chang, H.-L. Huang, H.-J. Chen, C.-H. Lai, C.-Y. Wen, Antibacterial properties and cytocompatibility of tantalum oxide coatings, Surf. Coat. Technol. 259 (2014) 193–198, http://dx.doi.org/10.1016/j.surfcoat.2014.03.061.
[23] M. Roy, V.K. Balla, S. Bose, A. Bandyopadhyay, Comparison of tantalum and hydroxyapatite coatings on titanium for applications in load bearing implants, Adv. Eng. Mater. 12 (2010) B637–B641, http://dx.doi.org/10.1002/adem.201080017.
[24] C. Persson, L. Guandalini, F. Baruffaldi, L. Pierotti, M. Baleani, Radiopacity of tantalum-loaded acrylic bone cement, Proc. Inst. Mech. Eng. H 220 (2006) 787–791.
[25] J. Black, Biologic performance of tantalum, Clin. Mater. 16 (1994) 167–173, http://dx.doi.org/10.1016/0267-6605(94)90113-9.
[26] F. ElBatal, G. El-Bassyouni, Bioactivity of Hench bioglass and corresponding glass-ceramic and the effect of transition metal oxides, SILICON 3 (2011) 185–197, http://dx.doi.org/10.1007/s12633-011-9095-6.
[27] L. Cordeiro, R.M. Silva, G.M. de Pietro, C. Pereira, E.A. Ferreira, S.J.L. Ribeiro, et al., Thermal and structural properties of tantalum alkali-phosphate glasses, J. Non-Cryst. Solids 402 (2014) 44–48, http://dx.doi.org/10.1016/j.jnoncrysol.2014.05.015.
[28] K.M. Wetherall, P. Doughty, G. Mountjoy, M. Bettinelli, A. Speghini, M.F. Casula, F. Cesare-Marincola, E. Locci, R.J. Newport, The atomic structure of niobium and tantalum containing borophosphate glasses, J. Phys. Condens. Matter 21 (2009) 37.
[29] A.M.F. Alhalawani, M.R. Towler, The effect of $ZnO \leftrightarrow Ta_2O_5$ substitution on the structural and thermal properties of SiO_2-ZnO-SrO-CaO-P_2O_5 glasses, Mater. Charact. 114 (2016) 218–224, http://dx.doi.org/10.1016/j.matchar.2016.03.004.
[30] O. Friberg, L.G. Dahlin, B. Söderquist, J. Källman, R. Svedjeholm, Influence of more than six sternal fixation wires on the incidence of deep sternal wound infection, Thorac. Cardiovasc. Surg. 54 (2006) 468–473, http://dx.doi.org/10.1055/s-2006-924437.
[31] D.J. Cohen, L.V. Griffin, A biomechanical comparison of three sternotomy closure techniques, Ann. Thorac. Surg. 73 (2002) 563–568.
[32] C. Schimmer, W. Reents, S. Berneder, P. Eigel, O. Sezer, H. Scheld, et al., Prevention of sternal dehiscence and infection in high-risk patients: a prospective randomized multicenter trial, Ann. Thorac. Surg. 86 (2008) 1897–1904, http://dx.doi.org/10.1016/j.athoracsur.2008.08.071.
[33] L.F. Lopez Almodovar, G. Bustos, P. Lima, A. Canas, I. Paredes, J.A. Buendia, Transverse plate fixation of sternum: a new sternal-sparing technique, Ann. Thorac. Surg. 86 (2008) 1016–1017, http://dx.doi.org/10.1016/j.athoracsur.2008.02.046.
[34] M. Ford, J. Brunelli, D. Song, P. Costello, R.M. Dunn, K. Billiar, Design of a screw-plate system to minimize loosening in sternal fixation, Bioeng. Conf. (NEBEC), 2011 IEEE 37th Annu. Northeast 2011, pp. 1–2, http://dx.doi.org/10.1109/NEBC.2011.5778555.
[35] P.W. Fedak, E. Kolb, G. Borsato, D.E. Frohlich, A. Kasatkin, K. Narine, et al., Kryptonite bone cement prevents pathologic sternal displacement, Ann. Thorac. Surg. 90 (2010) 979–985.
[36] P.W.M. Fedak, A. Kasatkin, Enhancing sternal closure using kryptonite bone adhesive: technical report, Surg. Innov. 18 (2011) NP8–N11, http://dx.doi.org/10.1177/1553350611412057.
[37] M. Holland, K. King, P. Fedak, Sternal closure with kryptonite - an innovative approach to a lingering pain in the chest, Can. J. Cardiol. 26 (2010) 269–282.
[38] C. Schimmer, M. Ozkur, B. Sinha, J. Hain, A. Gorski, B. Hager, et al., Gentamicin-collagen sponge reduces sternal wound complications after heart surgery: a controlled, prospectively randomized, double-blind study, J. Thorac. Cardiovasc. Surg. 143 (2012) 194–200, http://dx.doi.org/10.1016/j.jtcvs.2011.05.035.
[39] M.N. Mavros, P.K. Mitsikostas, V.G. Alexiou, G. Peppas, M.E. Falagas, Gentamicin collagen sponges for the prevention of sternal wound infection: a meta-analysis of randomized controlled trials, J. Thorac. Cardiovasc. Surg. 144 (2012) 1235–1240, http://dx.doi.org/10.1016/j.jtcvs.2012.06.040.
[40] S. Jolly, B. Flom, C. Dyke, Cabled butterfly closure: a novel technique for sternal closure, Ann. Thorac. Surg. 94 (2012) 1359–1361, http://dx.doi.org/10.1016/j.athoracsur.2012.05.067.
[41] A.W. Wren, A. Coughlan, L. Placek, M.R. Towler, Gallium containing glass polyalkenoate anti-cancerous bone cements: glass characterization and physical properties, J. Mater. Sci. Mater. Med. 23 (2012) 1823–1833, http://dx.doi.org/10.1007/s10856-012-4624-4.
[42] A.M.F. Alhalawani, L. Placek, A.W. Wren, D.J. Curran, D. Boyd, M.R. Towler, Influence of gallium on the surface properties of zinc based glass polyalkenoate cements, Mater. Chem. Phys. 147 (2014) 360–364, http://dx.doi.org/10.1016/j.matchemphys.2014.06.020.
[43] J.A. Williams, R.W. Billington, G.J. Pearson, The effect of the disc support system on biaxial tensile strength of a glass ionomer cement, Dent. Mater. 18 (2002) 376–379.
[44] ISO 9917-1:2007, Dentistry — Water-based cements — Part 1: Powder/Liquid Acid-base Cements, 2007.
[45] K.E. Kuettner, B.U. Pauli, G. Gall, V.A. Memoli, R.K. Schenk, Synthesis of cartilage matrix by mammalian chondrocytes in vitro. I. Isolation, culture characteristics, and morphology, J. Cell Biol. 93 (1982) 743–750.
[46] A.W. Wren, A. Kidari, N.M. Cummins, M.R. Towler, A spectroscopic investigation into the setting and mechanical properties of titanium containing glass polyalkenoate cements, J. Mater. Sci. Mater. Med. 21 (2010) 2355–2364, http://dx.doi.org/10.1007/s10856-010-4089-2.
[47] S.K. Tomlinson, O.R. Ghita, R.M. Hooper, K.E. Evans, Investigation of the dual setting mechanism of a novel dental cement using infrared spectroscopy, Vib. Spectrosc. 45 (2007) 10–17, http://dx.doi.org/10.1016/j.vibspec.2007.03.009.
[48] Y. Zhang, F. Zhu, J. Zhang, L. Xia, Converting layered zinc acetate nanobelts to one-dimensional structured ZnO nanoparticle aggregates and their photocatalytic activity, Nanoscale Res. Lett. 3 (2008) 201–204, http://dx.doi.org/10.1007/s11671-008-9136-2.
[49] S. Matsuya, Y. Matsuya, M. Ohta, Structure of bioactive glass and its application to glass ionomer cement, Dent. Mater. J. 18 (1999) 155–166.
[50] J. Rajamathi, S. Britto, M. Rajamathi, Synthesis and anion exchange reactions of a layered copper-zinc hydroxy double salt, $Cu_{1.6}Zn_{0.4}(OH)_3(OAc)\cdot H_2O$, J. Chem. Sci. 117 (2005) 629–633, http://dx.doi.org/10.1007/BF02708291.
[51] S. Matsuya, T. Maeda, M. Ohta, IR and NMR analyses of hardening and maturation of glass-ionomer cement, J. Dent. Res. 75 (1996) 1920–1927.
[52] M. Driessen, T. Miller, V. Grassian, Photocatalytic oxidation of trichloroethylene on zinc oxide: characterization of surface-bound and gas-phase products and intermediates with FT-IR spectroscopy, J. Mol. Catal. A Chem. 131 (1998) 149–156, http://dx.doi.org/10.1016/S1381-1169(97)00262-8.
[53] E.A. Wasson, J.W. Nicholson, Study on the setting chemistry of glass-ionomer cements, Clin. Mater. 7 (1991) 289–293.
[54] Toshiki Miyazaki, Hyun-Min Kim, Tadashi Kokubo, Hirofumi Kato, Takashi Nakamura, Induction and Acceleration of Bonelike Apatite Formation on Tantalum Oxide Gel in Simulated Body Fluid, J. Sol-Gel Sci. Technol. 21 (2001) 83–88.

[55] A.W. Wren, A. Coughlan, M.M. Hall, M.J. German, M.R. Towler, Comparison of a SiO_2–CaO–ZnO–SrO glass polyalkenoate cement to commercial dental materials: ion release, biocompatibility and antibacterial properties, J. Mater. Sci. Mater. Med. 24 (2013) 2255–2264, http://dx.doi.org/10.1007/s10856-013-4974-6.
[56] L. Grech, B. Mallia, J. Camilleri, Investigation of the physical properties of tricalcium silicate cement-based root-end filling materials, Dent. Mater. 29 (2013) e20–e28, http://dx.doi.org/10.1016/j.dental.2012.11.007.
[57] G.M. de Pietro, C. Pereira, R.R. Gonçalves, S.J.L. Ribeiro, C.D. Freschi, F.C. Cassanjes, et al., Thermal, structural, and crystallization properties of new tantalum alkali-germanate glasses, J. Am. Ceram. Soc. 98 (2015) 2086–2093, http://dx.doi.org/10.1111/jace.13555.
[58] A. Coughlan, K. Scanlon, B.P. Mahon, M.R. Towler, Zinc and silver glass polyalkenoate cements: an evaluation of their antibacterial nature, Biomed. Mater. Eng. 20 (2010) 99–106.
[59] Y.H. An, R.J. Friedman, Concise review of mechanisms of bacterial adhesion to biomaterial surfaces, J. Biomed. Mater. Res. 43 (1998) 338–348.
[60] A.W. Wren, A. Coughlan, F.R. Laffir, M.R. Towler, Comparison of a SiO_2-CaO-ZnO-SrO glass polyalkenoate cement to commercial dental materials: glass structure and physical properties, J. Mater. Sci. Mater. Med. 24 (2013) 271–280.
[61] A. Guida, M.R. Towler, J.G. Wall, Preliminary work on the antibacterial effect of strontium in glass ionomer cements, J. Mater. Sci. Lett. 22 (2003) 1401–1403.
[62] J.J. Harrison, M. Rabiei, R.J. Turner, E.A. Badry, K.M. Sproule, H. Ceri, Metal resistance in Candida biofilms, FEMS Microbiol. Ecol. 55 (2006) 479–491, http://dx.doi.org/10.1111/j.1574-6941.2005.00045.x.
[63] M.R. Bruins, S. Kapil, F.W. Oehme, Microbial resistance to metals in the environment, Ecotoxicol. Environ. Saf. 45 (2000) 198–207, http://dx.doi.org/10.1006/eesa.1999.1860.
[64] O.E. Sorensen, J.B. Cowland, K. Theilgaard-Monch, L. Liu, T. Ganz, N. Borregaard, Wound healing and expression of antimicrobial peptides/polypeptides in human keratinocytes, a consequence of common growth factors, J. Immunol. 170 (2003) 5583–5589.
[65] D.C. Smith, Development of glass-ionomer cement systems, Biomaterials 19 (1998) 467–478.
[66] A. Hoppe, N.S. Guldal, A.R. Boccaccini, A review of the biological response to ionic dissolution products from bioactive glasses and glass-ceramics, Biomaterials 32 (2011) 2757–2774, http://dx.doi.org/10.1016/j.biomaterials.2011.01.004.
[67] N. Moritz, E. Vedel, H. Ylanen, M. Jokinen, M. Hupa, A. Yli-Urpo, Characterisation of bioactive glass coatings on titanium substrates produced using a CO_2 laser, J. Mater. Sci. Mater. Med. 15 (2004) 787–794.